Hydrol. Earth Syst. Sci. Discuss., https://doi.org/10.5194/hess-2017-382
Manuscript under review for journal Hydrol. Earth Syst. Sci.
Discussion started: 4 July 2017

Hydrology and Earth System Sciences
Discussions

Time varying parameter models for catchments with land use change: the importance of model structure

Sahani Pathiraja[1], Daniela Anghileri[2], Paolo Burlando[2], Ashish Sharma[1], Lucy Marshall[1], Hamid Moradkhani[3]

[1]Water Research Centre
School of Civil and Environmental Engineering
University of New South Wales
Sydney, NSW
AUSTRALIA
Email: s.pathiraja@unsw.edu.au

[2]Institute of Environmental Engineering
ETH Zurich
Zurich
Switzerland

[3]Department of Civil and Environmental Engineering
Portland State University
Portland, Oregon
USA

Hydrol. Earth Syst. Sci. Discuss., https://doi.org/10.5194/hess-2017-382
Manuscript under review for journal Hydrol. Earth Syst. Sci.
Discussion started: 4 July 2017

Hydrology and Earth System Sciences
Discussions

Abstract

Rapid population and economic growth in South-East-Asia has been accompanied by extensive land use change with consequent impacts on catchment hydrology. Modelling methodologies capable of handling changing land use conditions are therefore becoming ever more important, and are receiving increasing attention from hydrologists. A recently developed Data Assimilation based framework that allows model parameters to vary through time in response to signals of change in observations is considered for a medium sized catchment (2880 km^2) in Northern Vietnam experiencing substantial but gradual land cover change. We investigate the efficacy of the method as well as the importance of the chosen model structure in ensuring the success of time varying parameter methods. The framework was utilized with two conceptual models (HBV and HyMOD) that gave good quality streamflow predictions during pre-change conditions. Although both time varying parameter models gave improved streamflow predictions under changed conditions compared to the time invariant parameter model, persistent biases for low flows were apparent in the HyMOD case. It was found that HyMOD was not suited to representing the modified baseflow conditions, resulting in extreme and unrealistic time varying parameter estimates. This work shows that the chosen model can be critical for ensuring the time varying parameter framework successfully models streamflow under changed land cover conditions. It also serves as an effective tool for separating the influence of climatic and land use change in retrospective studies where the lack of a paired control catchment precludes such an assessment.

Hydrol. Earth Syst. Sci. Discuss., https://doi.org/10.5194/hess-2017-382
Manuscript under review for journal Hydrol. Earth Syst. Sci.
Discussion started: 4 July 2017

Hydrology and Earth System Sciences
Discussions

1. Introduction

Population and economic growth in South-East Asia has led to significant land use change, with rapid deforestation occurring largely for agricultural purposes [*Kummer and Turner*, 1994]. Forest cover in the Greater Mekong Sub-region (comprising Myanmar, Thailand, Cambodia, Laos, Vietnam, and South China) has decreased from about 73% in 1973 to about 51% in 2009 [*WWF*, 2013]. Vietnam in particular has had the second highest rate of deforestation of primary forest in the world, based on estimates from the Forest Resource Assessment by the United Nations Food and Agriculture Organization [*FAO*, 2005]. Such extensive land use change has the potential to significantly alter catchment hydrology (in terms of both quantity and quality), with its effects sometimes not immediate but occurring gradually over a lengthy period of time. Recent estimates from satellite measurements indicate that rapid deforestation continues in the region, although at lower rates [e.g. *Kim et al.,* 2015]. Persistent land use change necessitates modelling methodologies that are capable of providing accurate hydrologic predictions, despite non-stationarity in catchment processes.

The literature on land-use change and its impacts on catchment hydrology is extensive, with studies examining the effects of 1) conversion to agricultural land-use [*Thanapakpawin et al*, 2007; *Warburton et al.,* 2012]; 2) deforestation [*Costa et al.,* 2003; *Coe et al*, 2011]; 3) afforestation [e.g. *Yang et al., 2012*; *Brown et al*, 2013] and urbanization [*Bhaduri et al.,* 2001; *Rose & Peters*, 2001]. Fewer studies have examined how traditional modelling approaches must be modified to handle non-stationary conditions, or how modelling methods can be used to assess impacts of land use change. Split sample calibration has been used frequently to retrospectively examine changes to model parameters due to land use or climatic change [*Seibert & McDonnell, 2010; Coron et al., 2012; McIntyre & Marshall*, 2010; *Legesse et al*, 2003]. Several other studies have employed scenario modelling, whereby hydrologic models are parameterized to represent different possible future land use conditions [e.g. *Niu & Sivakumar*, 2013; *Elfert & Borman*, 2010]. A related approach involves

45 combining land use change forecast models with hydrologic models [e.g. *Wijesekara et al.,* 2012].
46 However the aforementioned approaches are unsuited to short-term predictive modelling or
47 hydrologic forecasting in dynamic catchments, as the predicted land use change may not reflect
48 actual changes. A potentially more suitable approach in such a setting is to allow model parameters
49 to vary in time, rather than assuming a constant optimal value or stationary probability distribution.
50 Many existing methods utilising such a framework require some *apriori* knowledge of the land use
51 change in order to inform variations in model parameters (see for instance *Efstratiadis,* 2015; *Brown*
52 *et al.,* 2006; and *Westra et al.,* 2014). Recent efforts have examined the potential for time varying
53 models to automatically adapt to changing conditions using information contained in hydrologic
54 observations and sequential Data Assimilation, without requiring explicit knowledge of the changes
55 [see for example *Taver et al.,* 2015, *Pathiraja et al.,* 2016a&b]. Such approaches can objectively
56 modify model parameters in response to signals of change in observations in real time, whilst
57 simultaneously providing uncertainty estimates of parameters and streamflow predictions. They can
58 also be used to determine whether observed changes to streamflow dynamics are driven by climatic
59 or land cover changes.
60
61 *Pathiraja et al.* [2016a] presented an Ensemble Kalman Filter based algorithm (the so-called Locally
62 Linear Dual EnKF) to estimate time variations in model parameters. The method sequentially
63 assimilates observations into a numerical model to generate improved estimates of model states,
64 fluxes and parameters at a given time based on their respective uncertainties. The method was
65 applied to 2 sets of small (< 350 ha) paired experimental catchments with rapid and extensive
66 deforestation (50% and 100% of catchment cleared over 3 months), leading to strong signals of
67 change in the hydrologic observations [see *Pathiraja et al.,* 2016b]. Here we extend this work to a
68 larger catchment experiencing more realistic land cover change (more gradual and patchy), whilst
69 also investigating the importance of the chosen model structure. Previous studies have
70 demonstrated that impacts of land use change on the hydrologic response are dependent on many

71 factors including the type and rate of land cover conversion as well the spatial pattern of different
72 land uses within the catchment [*Dwarakish & Ganasri*, 2015; *Warburton et al.*, 2012]. In such
73 situations, the effects of unresolved spatial heterogeneities in model inputs (e.g. rainfall) and the
74 relatively less pronounced changes in land surface conditions make time varying parameter detection
75 more difficult. We also examine the role of the hydrologic model in determining the ability of the
76 time varying parameter framework to provide high quality predictions in changing conditions. These
77 issues are investigated for the Nammuc catchment (2880 km^2) in Northern Vietnam which has
78 experienced deforestation largely due to increasing agricultural development. Land cover change
79 has occurred at varying rates, with cropland accounting for roughly 23% between 1981 and 1994,
80 and 52% by 2000. We use two conceptual hydrologic models (given the availability of point rainfall,
81 temperature, and streamflow data) to determine the ability of the Locally Linear Dual EnKF to
82 produce accurate predictions under changing land surface conditions.
83
84 The remainder of this paper is structured as follows. Details of the study catchment and the impact
85 of land cover change are analysed in Section 2. Section 3 summarizes the experimental setup
86 including the hydrological models and the time varying parameter estimation method used. Results
87 are provided in Section 4, along with an analysis of whether the time varying model structures reflect
88 the observed catchment dynamics. Finally, we conclude with a summary of the main outcomes of
89 the study as well as proposed future work.

90 2. The Nammuc Catchment

91 The Nammuc catchment (2880 km^2) is located in the Red River Basin, the second largest drainage
92 basin in Vietnam which also drains parts of China and Laos. The local climate is tropical monsoon
93 dominated with distinct wet (May to October) and dry (November to April) seasons. The wet season
94 tends to have high temperatures (on average 27 to 29 °C) due to south-south easterly winds that
95 bring humid air masses. Conversely, during the dry season, circulation patterns reverse carrying

cooler dry air masses to the basin (leading to average temperatures of 16 to 21°C). Streamflow response is consequently monsoon driven, with high flows occurring between June and October (generally peaking in July/August) and low flows in the December to May period (Vu, 1993). Average annual rainfall at Nammuc varies between 1300 and 2000 mm (on average 1600 mm). A summary of catchment properties is provided in **Table 1**.

Figure 1 shows the available land cover information for the Nammuc catchment. The first land cover map refers to the period 1981-1994 and was obtained by the Vietnamese Forest Inventory and Planning Institute (http://fipi.vn/Home-en.htm). The second land cover map refers to year 2000 and was obtained from the FAO Global Land Cover database (http://www.fao.org/geonetwork/srv/en/metadata.show?id=12749&currTab=simple). A comparison of the two maps shows a reduction in forest cover in favor of cropland; Evergreen Leaf decreases from about 60% to 30% whilst cropland increases from about 23% to 52%. The change in land cover is patchy, although mostly concentrated in the northern part of the catchment. Because of the scant information available, it is not easy to identify the precise time period of these changes. Based on the available land cover map information and the changes to observed runoff (see **Section 2.1**), we posit that a period of rapid extensive deforestation occurred in early-1990s.

Daily point rainfall data is available at four precipitation stations surrounding the catchment (Dien Bien, Tuan Giao, Quynh Nhai and Nammuc, see **Figure 1**). Catchment averaged rainfall was developed as a weighted sum of the four stations with weights determined by Thiessen Polygons. Daily mean temperature was calculated in a similar fashion using temperature records from the 2 closest gauges (Lai Chau and Quynh Nhai, see **Figure 1**). This was used to estimate Potential Evapotranspiration through the empirical temperature-latitude based Hamon PET method [*Hamon*, 1961]. Daily rainfall, temperature and streamflow data was provided by the Vietnamese Institute of Water Resources Planning.

Hydrol. Earth Syst. Sci. Discuss., https://doi.org/10.5194/hess-2017-382
Manuscript under review for journal Hydrol. Earth Syst. Sci.
Discussion started: 4 July 2017

Hydrology and Earth System Sciences
Discussions

2.1.Impact of Land Cover Change on Streamflow

An examination of the observed streamflow and rainfall records shows that distinct changes to the hydrologic regime are evident after the mid-1990s. The annual runoff coefficient varies between 0.4 and 0.6 prior to 1994, after which it increases to between 0.6 and 0.8 until 2004 (see **Figure 2a**). However, increases to annual yields are driven mostly by changes to baseflow volume. This is evident in **Figure 2a**, which shows that the increase in the annual direct runoff coefficient $\left(\frac{runoff-baseflow}{rainfall}\right)$ is less than the increase in the total runoff coefficient (roughly 0.1 increase compared to 0.2 respectively). Baseflow was estimated using the two parameter recursive baseflow filter of *Eckhardt* [2005], with on-line updating of baseflow estimates to match low flows. A small increase in the Annual Baseflow Index $\left(\frac{baseflow}{runoff}\right)$ is apparent also, from about 0.32 on average in the period 1970 to 1982 to 0.39 on average after 1994 (**Figure 2b**). This indicates that the annual increases to baseflow volume exceed the increases to direct runoff volume. Similar changes were found by *Wang et al.* [2012] who analyzed records in the entire Da River basin which drains the largest river in the Red River catchment.

At a seasonal time scale, it is apparent that both wet and dry season flows exhibit temporal variations. We utilized the Moving Average Shifting Horizon (MASH) [*Anghileri et al.,* 2014] and Mann-Kendall test to assess seasonal trends in observed streamflow, precipitation, and temperature data. A steady increase in baseflow is again apparent (see February to April in **Figure 2c**), as well as increases to wet season flows (see June to September in **Figure 2c**). Mann-Kendall test (with significance level equal to 5%) on annual and monthly streamflow time series shows increasing trends in almost all months, i.e., from October to July. No concurrent increases are apparent in rainfall (see **Figure 2d**). Also the Mann-Kendall test applied to precipitation time series does not show any statistically significant trend, except a decrease in September for Nammuc and Quynh Nhai station and an increase in July for Dien Bien station. Temperature variations are not evident from the MASH analysis (not shown) and no significant trend can be detected by applying the Mann-Kendall

Hydrol. Earth Syst. Sci. Discuss., https://doi.org/10.5194/hess-2017-382
Manuscript under review for journal Hydrol. Earth Syst. Sci.
Discussion started: 4 July 2017

test. These results indicate that changes in streamflow dynamics are likely due to land use change rather than climatic impacts.

3. Experimental Setup

3.1.Hydrologic Models

Conceptual lumped models were adopted due to the availability of point rather than distributed hydro-meteorological data of sufficient length. We considered the HyMOD [*Boyle*, 2001] and Hydrologiska Byrans Vattenbalansavdelning (HBV) [*Bergstrom et al.,* 1995] models. They differ mainly in the way components of the response flow are separated (HBV has near surface flow, interflow, and baseflow components whilst HyMOD has a quickflow and slow flow component only) and how these flows are routed. A schematic of the models is shown in **Figure 3.**

In the HyMOD model, spatial variations in catchment soil storage capacity are represented by a Pareto distribution with shape parameter b and maximum point soil storage depth c_{max}. Excess rainfall (V) is partitioned into three cascading tanks representing quick flow and a single slow flow store through the splitting parameter α. Outflow from these linear routing tanks is controlled by parameters k_q (for the quick flow stores) and k_s (for the slow flow store). The model has a total of 5 states and 5 parameters.

In the HBV model, input to the soil store is represented by a power-law function (see **Figure 3**, note the snow store is neglected for this study). Excess rainfall enters a shallow layer store which generates: 1) near surface flow (q_0) whenever the shallow store state ($stw1$) is above a threshold ($hl1$) and 2) interflow (q_1) by a linear routing mechanism controlled by the $K1$ parameter. Percolation from the shallow layer store to the deep layer store (controlled by $perc$ parameter) then leads to the generation of baseflow also via linear routing (controlled by the $K2$ parameter). Finally, a

triangular weighting function of base length $Maxbas$ is used to route the sum of all three flow components. There are a total of 9 parameters and 3 states.

The Shuffled Complex Evolution Algorithm (SCE-UA) [*Duan et al.*, 1993] and the Borg Evolutionary Algorithm [*Hadka & Reed*, 2013] were used to calibrate the models to pre-change conditions (1973 to 1979). The period 1973 to 1979 was selected for calibration as it was expected to have minimal land cover changes, and also to ensure sufficient data availability for the assimilation period. Both models had very similar performance in terms of reproducing observed runoff (an NSE of 0.75 and 0.77 for HyMOD and HBV respectively). HBV was slightly better at reproducing low flows whilst HyMOD was slightly better at mid-range flows (see **Table 2**).

3.2. Time Varying Parameter Estimation

A framework for time varying parameter estimation based on Joint State and Parameter updating using the Ensemble Kalman Filter [*Evensen*, 1994] was presented in *Pathiraja et al.* [2016a]. The method works by sequentially proposing parameters, updating these using the Ensemble Kalman filter and available observations, and then using these updated parameters to propose and update model states. An approach for proposing parameters in the time varying setting was also presented, a task which is made difficult by the lack of a model that prescribes time variations in model parameters. The so-called Locally Linear Dual EnKF was verified against multiple synthetic case studies, as well as in 2 small experimental catchments experiencing controlled land use change [*Pathiraja et al.,* 2016b]. The algorithm is summarised below, for full details refer to *Pathiraja et al.* [2016a and 2016b].

Suppose a dynamical system can be described by a vector of states $\boldsymbol{x}_t$ and outputs $\boldsymbol{y}_t$ and a vector of associated model parameters $\boldsymbol{\theta}_t$ at any given time *t*. The uncertain system states and parameters are represented by an ensemble of states $\{\boldsymbol{x}_t^i\}_{i=1:n}$ and parameters $\{\boldsymbol{\theta}_t^i\}_{i=1:n}$ each with *n* members.

Suppose also that the system outputs are observed ($\boldsymbol{y}_t^o$) but that there is also some uncertainty associated with these observations. A single cycle of the Locally Linear Dual EnKF procedure for a given time *t* is undertaken as follows:

1. ***Propose a set of parameters.*** This involves generating a parameter ensemble using prior knowledge. In this case, our prior knowledge comes from the updated parameter ensemble from the previous time ($\boldsymbol{\theta}_{t-1}^{i+}$) and how it has changed over recent time steps. The prior (or background) ensemble ($\boldsymbol{\theta}_t^{i-}$) is generated by perturbing $\boldsymbol{\theta}_{t-1}^{i+}$with random noise such that its mean is a linear extrapolation of updated ensemble means from the previous two time steps. Perturbations are sampled from a Gaussian density with mean zero and variance $s^2\boldsymbol{\Sigma}_{t-1}^{\theta}$, where $\boldsymbol{\Sigma}_{t-1}^{\theta}$ is the covariance matrix of the updated parameter ensemble from the previous time and s^2 is a tuning parameter. The ensemble mean is then shifted to ensure it matches the linear extrapolation. Note that the extrapolation is forced to be less than a pre-defined maximum rate of change to minimise overfitting and avoid parameter drift due to isolated large updates.
2. ***Consider observation and forcing uncertainty.*** This is done by perturbing measurements of forcings and system outputs with random noise sampled from a distribution representing the errors in those measurements. The result is an ensemble of forcings ($\boldsymbol{u}_t^i$) and observations ($\boldsymbol{y}_t^i$) each with *n* members.
3. ***Generate simulations using prior parameters***. The prior parameters from Step 1 and updated states from the previous time are forced through the model equations to generate an ensemble of model simulations of states ($\hat{\boldsymbol{x}}_t^i$) and outputs ($\hat{\boldsymbol{y}}_t^i$).
4. ***Perform the Kalman update of parameters.*** Parameters are updated using the Kalman update equation and the prior parameter and simulated output ensemble from Step 1 and 3

$$\boldsymbol{\theta}_t^{i+} = \boldsymbol{\theta}_t^{i-} + \mathbf{K}_t^{\theta}\left(\boldsymbol{y}_t^i - \hat{\boldsymbol{y}}_t^i\right) \; for\; i = 1{:}n \quad (1)$$

$$\mathbf{K}_t^{\theta} = \boldsymbol{\Sigma}_t^{\theta\hat{y}}\left[\boldsymbol{\Sigma}_t^{\hat{y}\hat{y}} + \boldsymbol{\Sigma}_t^{y^o y^o}\right]^{-1} \quad (2)$$

where $\boldsymbol{\Sigma}_t^{\theta\hat{y}}$ is a matrix of the cross covariance between errors in parameters $\boldsymbol{\theta}_t^{i-}$ and simulated observations $\hat{\boldsymbol{y}}_t^i$; $\boldsymbol{\Sigma}_t^{y^o y^o}$ is the error covariance matrix of the observations; and $\boldsymbol{\Sigma}_t^{\hat{y}\hat{y}}$ is the error covariance matrix of the simulated observations.

5. ***Generate simulations using updated parameters.*** Step 3 is repeated with the updated parameter ensemble $\boldsymbol{\theta}_t^{i+}$ to generate an ensemble of model simulations of states ($\boldsymbol{x}_t^{i-}$) and outputs ($\tilde{\boldsymbol{y}}_t^i$).

6. ***Perform the Kalman update of states and outputs***. Use the Kalman update equation for correlated measurement and process noise, and the simulated state ($\boldsymbol{x}_t^{i-}$) and output ($\tilde{\boldsymbol{y}}_t^i$) ensembles from Step 5 to update them:

$$\boldsymbol{x}_t^{i+} = \boldsymbol{x}_t^{i-} + \mathbf{K}_t^x\left(\boldsymbol{y}_t^i - \tilde{\boldsymbol{y}}_t^i\right) \; for \; i = 1{:}n \quad (3)$$

$$\mathbf{K}_t^x = \left[\boldsymbol{\Sigma}_t^{x\tilde{y}} + \boldsymbol{\Sigma}_t^{\varepsilon_x y^o}\right]\left[\boldsymbol{\Sigma}_t^{\tilde{y}\tilde{y}} + \boldsymbol{\Sigma}_t^{\varepsilon_{\tilde{y}} y^o} + \left(\boldsymbol{\Sigma}_t^{\varepsilon_{\tilde{y}} y^o}\right)^{\mathbf{T}} + \boldsymbol{\Sigma}_t^{y^o y^o}\right]^{-1} \quad (4)$$

$$\boldsymbol{\varepsilon}_{x_t}{}^i = \boldsymbol{x}_t^{i-} - \hat{\boldsymbol{x}}_t^i \; ; \; \boldsymbol{\varepsilon}_{\tilde{y}_t}{}^i = \tilde{\boldsymbol{y}}_t^i - \hat{\boldsymbol{y}}_t^i \quad (5)$$

where $\boldsymbol{\Sigma}_t^{x\tilde{y}}$ is a matrix of the cross covariance between simulated states $\left\{\boldsymbol{x}_t^{i-}\right\}_{i=1:n}$ and outputs $\left\{\tilde{\boldsymbol{y}}_t^i\right\}_{i=1:n}$ from Step 5; $\boldsymbol{\Sigma}_t^{\varepsilon_x y^o}$ represents the covariance between $\left\{\boldsymbol{\varepsilon}_{x_t}{}^i\right\}_{i=1:n}$ and the observations; $\boldsymbol{\Sigma}_t^{\varepsilon_{\tilde{y}} y^o}$ represents the covariance between the $\left\{\boldsymbol{\varepsilon}_{\tilde{y}_t}{}^i\right\}_{i=1:n}$ and the observations; and $(\,)^{\mathbf{T}}$ represents the transpose operator.

3.2.1. Application to the Nammuc Catchment

Joint state and parameter estimation was undertaken for the Nammuc Catchment over the period 1975 to 2004 by assimilating streamflow observations into the HyMOD and HBV models at a daily time step. Given the fairly low parameter dimensionality of HyMOD, all model parameters were allowed to vary in time whilst for HBV the lp and $Maxbas$ parameters (see **Figure 3**) were held fixed (lp = 1 and $Maxbas$ = 1 day). This was based on the results of Variance Based Sensitivity Analysis or Sobol method [see for example *Saltelli et al.,* 2008] implemented through the SAFE toolbox [*Pianosi*

et al., 2015] which found these to be the least sensitive and least important in defining variations to catchment hydrology (see **Table 3**). Note that although the $hl1$ parameter was found to have low sensitivity, it was retained as a time varying parameter due to its conceptual importance in separating interflow and near surface flow (refer **Figure 3**).

Unbiased normally distributed ensembles of the parameters and states are required to initialise the LL Dual EnKF. Initial parameter ensembles were generated by sampling from a Gaussian distribution with mean equal to the calibrated parameters over the pre-change period and variance estimated from parameter sets with similar objective function values. Parameter sets with similar objective function values were obtained when using different starting points to the optimization algorithm during the model calibration stage. Initial state ensembles were also sampled from normal distributions with mean equal to the simulated state at the end of the calibration period. An ensemble size of 100 members was adopted and assumed sufficiently large based on the findings of *Moradkhani et al.* [2005] and *Aksoy et al.* [2006]. Due to the stochastic-dynamic nature of the method, ensemble statistics were calculated over 20 separate realisations of the LL Dual EnKF. The prior parameter generating method described in Step 1 of **Section 3.2** requires specification of the tuning parameter s^2 to define the variance of the perturbations. This was tuned by selecting the s^2 value that optimized the log score [*Good,* 1952] (a measure of forecast quality) of background streamflow predictions ($\tilde{\boldsymbol{y}}_t^i$) obtained from the LL Dual EnKF. The maximum allowable daily rate of change in the ensemble mean was based on assuming a linear rate of change within the entire feasible parameter space over a three year period.

As detailed in **Section 3.2**, observation and forcing uncertainty is considered by perturbing measurements with random noise. Here streamflow errors were assumed to be zero-mean normally distributed (truncated to ensure positivity) and heteroscedastic. The variance is defined as a

Hydrol. Earth Syst. Sci. Discuss., https://doi.org/10.5194/hess-2017-382
Manuscript under review for journal Hydrol. Earth Syst. Sci.
Discussion started: 4 July 2017

Hydrology and Earth System Sciences
Discussions

proportion of the observed streamflow, to reflect the fact that larger flows tend to have greater errors than low flows:

$$q_{obs}^{i}(t) = q_{obs}(t) + \varepsilon_q^i \ where\ \varepsilon_q^i \sim TN\left(0, d \text{ x } q_{obs}(t)\right) \quad i = 1{:}n \qquad (6)$$

where TN indicates the truncated normal distribution to ensure positive flows and d = 0.1. A multiplier of 0.1 was chosen based on estimates adopted for similar gauges in hydrologic DA studies [e.g. *Clark et al.,* 2008; *Weerts & Serafy,* 2006; *Xie et al.,* 2014].

Several studies have noted that a major source of rainfall uncertainty arises from scaling point rainfall to the catchment scale [*Villarini & Krajewski*, 2008; *McMillan et al.*, 2011] and that multiplicative errors models are suited to describing such errors [e.g. *Kavetski et al.*, 2006]. Rainfall uncertainties were therefore described using unbiased, lognormally distributed multipliers:

$$P^i(t) = P(t).M^i \qquad (7)$$

$$M^i \sim LN(m, v) \text{ and } X^i = \log\left(M^i\right) \sim N(\mu, \sigma^2) \qquad i = 1{:}n \qquad (8)$$

where m and v are the mean and variance of the lognormally distributed rainfall multipliers M respectively and μ and σ^2 are the mean and variance of the normally distributed logarithm of the rainfall multipliers M. For unbiased perturbations, we let m = 1. The variance of the rainfall multipliers (v) was estimated by considering upper and lower bound error estimates in the Thiessen weights assigned to the four rainfall stations (see Section 2 for calculation of catchment averaged rainfall, $P(t)$). The resulting upper and lower bound catchment averaged rainfall sequences were then used to estimate error parameters due to spatial variation in rainfall:

$$v = e^{(2\mu + \sigma^2)}.\left(e^{\sigma^2} - 1\right) \qquad (9)$$

$$\sigma^2 = \widehat{\sigma^2} = var\left(\log\left[\frac{\boldsymbol{P}_{upper,10}}{\boldsymbol{P}_{lower,10}}\right]\right) \qquad (10)$$

$$\mu = \log(m) - \frac{\sigma^2}{2} = -\frac{\sigma^2}{2} \qquad (11)$$

where $\boldsymbol{P}_{upper,10}$ indicates catchment averaged rainfall sequence using the upper bound Thiessen weights with daily depth greater than 10mm (similar for $\boldsymbol{P}_{lower,10}$) and $\widehat{\sigma^2}$ was found to be 0.05. A

Hydrol. Earth Syst. Sci. Discuss., https://doi.org/10.5194/hess-2017-382
Manuscript under review for journal Hydrol. Earth Syst. Sci.
Discussion started: 4 July 2017

10mm rainfall depth threshold was chosen to avoid large rainfall fractions due to small rainfall depths. Similarly, we assume the dominant source of uncertainty in temperature data arises from spatial variation. Differences in temperature records at Lai Chau and Quynh Nhai (only available gauges with temperature records) were analysed and found to be approximately normally distributed with sample mean 0.2 deg C and variance of 1.4 deg C. A perturbed temperature ensemble was then generated according to equation 13:

$$T^i(t) = T_{avg}(t) + \varepsilon_T^i \ \ where\ \varepsilon_T^i \sim TN(0, 1.4) \qquad i = 1{:}n \qquad (12)$$

where $T_{avg}(t)$ represents catchment averaged temperature (see Section 2). Note that perturbations were taken to be unbiased (zero mean) as the sample mean of the differences in the temperature records was close to zero. The same perturbed input and observation sequences were used for the HyMOD and HBV runs for the sake of comparison. A summary of the values adopted for the various components of the Locally Linear Dual EnKF for each model is provided in **Table 4 and 5.**

4. Results and Discussion

Variations in the estimated parameter distributions from the LL Dual EnKF are evident for both models. In the case of the HBV model, changes at an inter-annual time scale are evident for the $perc$ and β (see **Figure 4**). The decrease in the β parameter means that a greater proportion of rainfall is converted to runoff (i.e. more water entering the shallow layer storage). Additionally, the increase in the $perc$ parameter means that a greater volume of water is made available for baseflow generation. These changes correspond with the observed increase in the annual runoff coefficient (**Figure 2**) and increase in baseflow volume (as discussed in **Section 2.1**). Similar parameter adjustments are seen for HyMOD, at least at a qualitative level (see **Figure 5**). The sharp increase in the b parameter during the post-change period means that a greater volume of water is available for routing (as larger b values mean that a smaller proportion of the catchment has deep soil storage capacity) and the downward inter-annual trend in α means that a greater portion of excess runoff is

routed through the baseflow store. Intra-annual variations in updated model parameters for both HyMOD and HBV are also apparent (refer **Figures 4 and 5**). This is due to the inability of a single parameter distribution to accurately model both wet and dry season flows, an issue that is commonly encountered when modelling large heterogeneous catchments experiencing significant spatial variation in rainfall. Such variations were not observed when using the time varying parameter framework for small deforested catchments (< 350ha) [see *Pathiraja et al.,* 2016b]. The comparatively less clear parameter changes for the Nammuc catchment are due to a combination of the increased difficulty in accurately modelling the hydrologic response (even in pre-change conditions) and due to the relatively more subtle and gradual changes to land cover. Nonetheless, the method is shown to generate a temporally varying structure that is conceptually representative of the observed changes.

Despite the overall correspondence between changes to model parameters and observed streamflow, a closer examination shows that the hydrologic model structure is critical in determining whether the time varying parameter models accurately reflect changes in all aspects of the hydrologic response (not just total streamflow). In order to examine the impact of parameter variations on the model dynamics, we generated model simulations with the time varying parameter ensemble from the LL Dual EnKF, but without state updating (hereafter referred to as TVP-HBV and TVP-HyMOD). Streamflow predictions from the LL Dual EnKF (i.e. with state and parameter updating) for both the HyMOD and HBV are generally of similar quality and superior to those from the respective time invariant parameter models, although a slight bias in baseflow predictions from HyMOD is evident (see for example **Figure 6**). However, differences in predictions from TVP-HBV and TVP-HyMOD are more striking due to the lack of state updating. **Figure 7** shows annual statistics of simulated streamflow from the TVP-HBV and TVP-HyMOD models and observed runoff. The TVP-HBV gives direct runoff and baseflow predictions that are consistent with runoff observations, meaning that the parameter adjustments reflect the observed changes in the runoff response. This

however is not the case for the TVP-HyMOD. The annual runoff coefficient and annual direct runoff coefficient are severely under-estimated in the post-change period by the TVP-HyMOD, whilst the Annual Baseflow Index has an increasing trend of magnitude far greater than observed (**Figure 7c**). All three quantities on the other hand are well represented by the TVP-HBV (**Figure 7**).

Similar conclusions can be drawn from **Figure 8**, which shows the results of a Moving Average Shifting Horizon (MASH) analysis (see **Section 2.1**) on total and direct runoff (observed and simulated). Observed increases in January to April flows (see **Figure 8a**) and wet season direct flows (July to September) (see **Figure 8e**) are well represented by the TVP-HBV but not TVP-HyMOD. The reason for these differences between the two models lies in their structure. In joint state-parameter updating using HyMOD, underestimated runoff predictions during recession periods lead to adjustments to the k_s and α parameters to increase baseflow depth. Unlike HBV, HyMOD has no continuous supply of water to the routing stores (i.e. the quick flow and slow flow stores) during recession periods (which typically have extended periods of no rainfall, so that V in **Figure 3** is zero). This means that k_s and α are updated to extreme values to compensate for the volumetric shortfall. HBV on the other hand has a continuous percolation of water into the deep layer store even during periods of no rain (so long as the shallow water store is non-empty). In summary, the HyMOD model structure prevents the parameters from being updated to values that realistically reflect the observed changes to catchment dynamics.

Having established that the TVP-HBV provided a good representation of the observed streamflow dynamics, we used a modelling approach to determine whether the observed changes were climatically driven and which (if any) components of runoff were affected by land use change. A resampled rainfall and temperature time series was generated by sampling the data without replacement across years for each day (for instance rainfall and temperature for 1st January 1990 is found by randomly sampling from all records on 1st January). This maintains the intra-annual (e.g.

seasonal) variability but destroys any inter-annual trends in the meteorological data. Streamflow simulations were then generated using this resampled meteorological sequence as inputs to the TVP-HBV (i.e. without state updating). **Figure 8d**&**h** show the results of a MASH undertaken on the resulting simulations of total and direct runoff. Observed increases in baseflow during the January – April period (see **Figure 8a**) and increases in direct runoff in the June – September period (see **Figure8e**) are reproduced. The magnitude of increase in direct runoff in July is slightly lower, indicating the potential for some climatic influences also. This is consistent with findings from the Mann-Kendall test which identified a statistically significant increase in July rainfall (see Section 2.1). Overall however, these results lend further weight to the conclusion that land cover change has impacted the hydrologic regime of the Nammuc catchment.

5. Conclusions

As our anthropogenic footprint expands, it will become increasingly important to develop modelling methodologies that are capable of handling dynamic catchment conditions. Previous work proposed the use of models whose parameters vary with time in response to signals of change in observations. The so-called Locally Linear Dual EnKF time varying parameter estimation algorithm [*Pathiraja et al.,* 2016a] was applied to 2 sets of small (< 350 ha) paired experimental catchments with deforestation occurring under experimental conditions (rapid clearing of 100% and 50% of land surface) [*Pathiraja et al.,* 2016b]. Here we demonstrate the efficacy of the method for a larger catchment experiencing more realistic land cover change, whilst also investigating the importance of the chosen model structure in ensuring the success of time varying parameter methods. We also demonstrate that the time varying parameter framework can be used in a retrospective fashion to determine whether changes to the hydrologic regime are a result of climatic or land cover changes.

Experiments were undertaken on the Nammuc catchment (2880 km^2) in Vietnam, which experienced a relatively gradual conversion from forest to cropland over a number of years (cropland increased

394 from roughly 23% of the catchment between 1981 and 1994 to 52% by 2000). Changes to the
395 hydrologic regime after the mid-1990s were detected and attributed mostly to an increase in
396 baseflow volume. Application of the LL Dual EnKF with two conceptual models (HBV and HyMOD)
397 showed that the time varying parameter framework with state updating improved streamflow
398 prediction in post-change conditions compared to the time invariant parameter case. However,
399 baseflow predictions from the LL Dual EnKF with HBV were generally superior to the HyMOD case
400 which tended to have a slight negative bias. It was found that the structure (i.e. model equations) of
401 HyMOD was unsuited to representing the modified baseflow conditions, resulting in extreme and
402 unrealistic time varying parameter estimates. This work shows that the chosen model is critical for
403 ensuring the time varying parameter framework successfully models streamflow in unknown future
404 land cover conditions. Appropriate model selection can be a difficult task due to the significant
405 uncertainty associated with future land use change, and can be even more problematic when
406 multiple models have similar performance in pre-change conditions (as was the case in this study).
407 One possible way to ensure success of the time varying parameter approach is to use physically
408 based models whose fundamental equations more closely model physical processes (for instance,
409 modelling sub-surface flow using Richard's equation with hydraulic conductivity allowed to vary with
410 time). The drawback of such approaches is that they are generally data intensive, both in generating
411 model simulations (i.e. detailed inputs) and specifying parameters. Another possibility is to combine
412 time varying parameter framework with multi-model approaches.

413 ## 6. Acknowledgements

414 This study was funded by the Australian Research Council as part of the Discovery Project
415 DP140102394. Dr Marshall is additionally supported through a Future Fellowship FT120100269.
416
417 The data used in this paper were collected under the project IMRR (Integrated and sustainable water
418 Management of Red Thai Binh Rivers System in changing climate), funded by the Italian Ministry of

419 Foreign Affairs (Delibera n. 142 del 8 Novembre 2010). We greatly acknowledge Dr. Andrea
420 Castelletti for provision of data and for discussions on this work.

421

422 Data utilized in this study can be made available from the authors upon request.

7. References

Aksoy, A., Zhang, F., Nielsen-Gammon, J. (2006). Ensemble-Based Simultaneous State and Parameter Estimation in a Two-Dimensional Sea-Breeze Model. *Monthly Weather Review*, 134, 2951–2970.

Anghileri, D., Pianosi, F., & Soncini-Sessa, R. (2014). Trend detection in seasonal data: From hydrology to water resources. *Journal of Hydrology*, *511*, 171–179. http://doi.org/10.1016/j.jhydrol.2014.01.022

Bergström, S. 1995. The HBV model. In: Singh, V.P. (Ed.) *Computer Models of Watershed Hydrology*. Water Resources Publications, Highlands Ranch, CO., pp. 443-476.

Bhaduri, B. B., Minner, M., Tatalovich, S., Member, A., & Harbor, J. (2001). Long-term hydrologic impact of urbanization: A tale of two models. *Journal of Water Resources Planning and Management*, *127*(February), 13–19.

Boyle, D. (2001). Multicriteria calibration of hydrological models, *Ph.D. dissertation*, Univ. of Ariz., Tucson.

Brown, A. E., Mcmahon, T. A., Podger, G. M., & Zhang, L. (2006). A methodology to predict the impact of changes in forest cover on flow duration curves, *CSIRO Land and Water Science Report 8/06*.

Brown, A. E., Western, A. W., McMahon, T. a., & Zhang, L. (2013). Impact of forest cover changes on annual streamflow and flow duration curves. *Journal of Hydrology*, *483*, 39–50. http://doi.org/10.1016/j.jhydrol.2012.12.031

Clark, M. P., Rupp, D. E., Woods, R. A., Zheng, X., Ibbitt, R. P., Slater, A. G., … Uddstrom, M. J. (2008). Hydrological data assimilation with the ensemble Kalman filter: Use of streamflow observations to update states in a distributed hydrological model. *Advances in Water Resources*, *31*(10), 1309–1324. http://doi.org/10.1016/j.advwatres.2008.06.005

Coe, M. T., Latrubesse, E. M., Ferreira, M. E., & Amsler, M. L. (2011). The effects of deforestation and climate variability on the streamflow of the Araguaia River, Brazil. *Biogeochemistry*, *105*(1–3), 119–131. http://doi.org/10.1007/s10533-011-9582-2

Coron, L., Andréassian, V., Perrin, C., Lerat, J., Vaze, J., Bourqui, M., & Hendrickx, F. (2012). Crash testing hydrological models in contrasted climate conditions: An experiment on 216 Australian catchments. *Water Resources Research,* 48(5), 1–17. doi:10.1029/2011WR011721

Costa, M. H., Botta, A., & Cardille, J. A. (2003). Effects of large-scale changes in land cover on the discharge of the Tocantins River, Southeastern Amazonia. *Journal of Hydrology*, *283*(1–4), 206–217. http://doi.org/10.1016/S0022-1694(03)00267-1

Duan, Q. Y., Gupta, V. K., & Sorooshian, S. (1993). Shuffled complex evolution approach for effective and efficient global minimization. *Journal of Optimization Theory and Applications*, *76*(3), 501–521. doi:10.1007/BF00939380

Dwarakish, G. S., & Ganasri, B. P. (2015). Impact of land use change on hydrological systems: A review of current modeling approaches. *Cogent Geoscience*, *1*(1), 1115691–1115691. http://doi.org/10.1080/23312041.2015.1115691

460 Eckhardt, K. (2005). How to construct recursive digital filters for baseflow separation. *Hydrological*
461 *Processes*, *19*(2), 507–515. http://doi.org/10.1002/hyp.5675

462 Efstratiadis, A., Nalbantis, I., & Koutsoyiannis, D. (2015). Hydrological modelling of temporally-varying
463 catchments: facets of change and the value of information. *Hydrological Sciences Journal*, *60*(7–
464 8), 1438–1461. http://doi.org/10.1080/02626667.2014.982123

465 Elfert, S., & Bormann, H. (2010). Simulated impact of past and possible future land use changes on
466 the hydrological response of the Northern German lowland "Hunte" catchment. *Journal of*
467 *Hydrology*, 383, 245–255. http://dx.doi.org/10.1016/j.jhydrol.2009.12.040

468 Evensen, G. (1994). Sequential data assimilation with a nonlinear quasi-geostrophic model using
469 Monte Carlo methods to forecast error statistics. *Journal of Geophysical Research*, *99*(C5).
470 http://doi.org/10.1029/94JC00572

471 FAO (2005). Global Forest Resources Assessment 2005 (FRA 2005)

472 Good, I.J. (1952). Rational Decisions. *Journal of the Royal Statistical Society.* B 14: 107–114.
473
474 Hadka, D., Reed, P., (2013). Borg: an auto–adaptive many–objective evolutionary computing
475 framework. *Evol. Comput*. 21 (2), 231–259.

476 Hamon, W. (1961). Estimating potential evapotranspiration. *Transactions of the American Society of*
477 *Civil Engineers*, 128(1), pp.324-337.

478 Kavetski, D., Kuczera, G., & Franks, S. W. (2006). Bayesian analysis of input uncertainty in hydrological
479 modeling: 1. Theory. *Water Resources Research*, *42*(3), n/a–n/a. doi:10.1029/2005WR004368
480
481 Kim, D.-H., J. O. Sexton, and J. R. Townshend (2015). Accelerated deforestation in the humid tropics
482 from the 1990s to the 2000s, *Geophysical Research Letters*, 42, 3495–3501, doi:10.1002/
483 2014GL062777.

484
485 Kummer, D., and Turner, B. (1994). The Human Causes of Deforestation in Southeast Asia. *BioScience,*
486 *44*(5), 323-328. doi:10.2307/1312382
487
488 Legesse, D., Vallet-Coulomb, C., & Gasse, F. (2003). Hydrological response of a catchment to climate
489 and land-use changes in Tropical Africa: case study South Central Ethiopia. *Journal of Hydrology*,
490 *275*(1-2), 67–85. doi:10.1016/S0022-1694(03)00019-2
491
492 McIntyre, N., & Marshall, M. (2010). Identification of rural land management signals in runoff
493 response. *Hydrological Processes*, *24*(24), 3521–3534. doi:10.1002/hyp.7774
494
495 McMillan, H., Jackson, B., Clark, M., Kavetski, D., & Woods, R. (2011). Rainfall uncertainty in
496 hydrological modelling: An evaluation of multiplicative error models. *Journal of Hydrology*,
497 *400*(1-2), 83–94. doi:10.1016/j.jhydrol.2011.01.026

498 Moradkhani, H., Sorooshian, S., Gupta, H. V., & Houser, P. R. (2005). Dual state–parameter
499 estimation of hydrological models using ensemble Kalman filter. *Advances in Water Resources*,
500 *28*(2), 135–147. http://doi.org/10.1016/j.advwatres.2004.09.002

Niu, J., & Sivakumar, B. (2013). Study of runoff response to land use change in the East River basin in South China. *Stochastic Environmental Research and Risk Assessment*. doi:10.1007/s00477-013-0690-5

Pathiraja, S., Marshall, L., Sharma, A., & Moradkhani, H. (2016a). Hydrologic modeling in dynamic catchments: A data assimilation approach. *Water Resources Research*, *52*, 3350–3372. http://doi.org/10.1002/2015WR017192

Pathiraja, S., Marshall, L., Sharma, a., & Moradkhani, H. (2016b). Detecting non-stationary hydrologic model parameters in a paired catchment system using data assimilation. *Advances in Water Resources*, *94*, 103–119. http://doi.org/10.1016/j.advwatres.2016.04.021

Pianosi, F., Sarrazin, F., Wagener, T. A Matlab toolbox for Global Sensitivity Analysis, *Environmental Modelling & Software*, 70, 80-85, http://dx.doi.org/10.1016/j.envsoft.2015.04.009.

Rose, S., & Peters, N. E. (2001). Effects of urbanization on streamflow in the Atlanta area (Georgia, USA): a comparative hydrological approach. *Hydrological Processes*, *15*(8), 1441–1457. http://doi.org/10.1002/hyp.218

Saltelli, A., Ratto, M., Andres, T., Campolongo, F., Cariboni, J., Gatelli, D., Saisana, M., Tarantola, S., (2008). Global Sensitivity Analysis, the Primer. Wiley.

Seibert, J., & McDonnell, J. J. (2010). Land-cover impacts on streamflow: a change-detection modelling approach that incorporates parameter uncertainty. *Hydrological Sciences Journal*, *55*(3), 316–332. doi:10.1080/02626661003683264

Taver, V., Johannet, a., Borrell-Estupina, V., & Pistre, S. (2015). Feed-forward vs recurrent neural network models for non-stationarity modelling using data assimilation and adaptivity. *Hydrological Sciences Journal*, *60*(7–8), 1242–1265. http://doi.org/10.1080/02626667.2014.967696

Thanapakpawin, P., Richey, J., Thomas, D., Rodda, S., Campbell, B., & Logsdon, M. (2007). Effects of landuse change on the hydrologic regime of the Mae Chaem river basin, NW Thailand. *Journal of Hydrology*, *334*(1-2), 215–230. doi:10.1016/j.jhydrol.2006.10.012

Villarini, G., & Krajewski, W. F. (2008). Empirically-based modeling of spatial sampling uncertainties associated with rainfall measurements by rain gauges. *Advances in Water Resources*, *31*(7), 1015–1023. doi:10.1016/j.advwatres.2008.04.007

Vu, V.T., 1993. Evaluation of the impact of deforestation to inflow regime of the Hoa Binh Reservoir in Vietnam, Hydrology of Warm Humid Regions (Proceedings of the Yokohama Symposium, July 1993). IAHS Publ. no. 216

Wang, J., Ishidaira, H., & Xu, Z. X. (2012). Effects of climate change and human activities on inflow into the Hoabinh Reservoir in the Red River basin. *Procedia Environmental Sciences*, *13*, 1688-1698.

Warburton, M. L., Schulze, R. E., & Jewitt, G. P. W. (2012). Hydrological impacts of land use change in three diverse South African catchments. *Journal of Hydrology*, *414–415*, 118–135. http://doi.org/10.1016/j.jhydrol.2011.10.028

542 Weerts, A. H., & El Serafy, G. Y. H. (2006). Particle filtering and ensemble Kalman filtering for state
543 updating with hydrological conceptual rainfall-runoff models. *Water Resources Research*, *42*(9),
544 n/a-n/a. http://doi.org/10.1029/2005WR004093

545 Westra, S.; Thyer, M.; Leonard, M.; Kavetski, D.; Lambert, M. (2014). A strategy for diagnosing and
546 interpreting hydrological model nonstationarity. *Water Resources Research*, 5090–5113.
547 http://doi.org/10.1002/2013WR014719.Received

548 Wijesekara, G. N., Gupta, A., Valeo, C., Hasbani, J. G., Qiao, Y., Delaney, P., & Marceau, D. J. (2012).
549 Assessing the impact of future land-use changes on hydrological processes in the Elbow River
550 watershed in southern Alberta, Canada. *Journal of Hydrology*, *412–413*, 220–232.
551 http://doi.org/10.1016/j.jhydrol.2011.04.018

552 WWF. (2013). Ecosystems in the Greater Mekong: Past trends, current status, possible futures.

553 Xie, X., Meng, S., Liang, S., & Yao, Y. (2014). Improving streamflow predictions at ungauged locations
554 with real-time updating: application of an EnKF-based state-parameter estimation strategy.
555 *Hydrology and Earth System Sciences*, *18*(10), 3923–3936. http://doi.org/10.5194/hess-18-
556 3923-2014

557 Yang, L., Wei, W., Chen, L., & Mo, B. (2012). Response of deep soil moisture to land use and
558 afforestation in the semi-arid Loess Plateau, China. *Journal of Hydrology*, *475*, 111–122.
559 http://doi.org/10.1016/j.jhydrol.2012.09.041

Hydrol. Earth Syst. Sci. Discuss., https://doi.org/10.5194/hess-2017-382
Manuscript under review for journal Hydrol. Earth Syst. Sci.
Discussion started: 4 July 2017

Hydrology and Earth System Sciences
Open Access
EGU
Discussions

560 # Tables

	Pre 1994	Post 1994
	Land Use	
Evergreen Forest (including evergreen needle and evergreen leaf) (%)	77%	48%
Cropland (%)	23%	52%
	Hydro-Meteorological Properties	
Mean Annual Rainfall (mm)	1630	1660
Mean Annual Runoff (mm)	838	1190
Mean Annual Runoff Coefficient	0.5	0.7
Mean Annual PET (mm)	1300	1300

561 **Table 1: Study Catchment Properties**

562

563

564

Hydrol. Earth Syst. Sci. Discuss., https://doi.org/10.5194/hess-2017-382
Manuscript under review for journal Hydrol. Earth Syst. Sci.
Discussion started: 4 July 2017

565

	HYMOD	HBV
NSE [ ]	**0.77**	0.75
Peak flows (q > 5mm/d)		
MAE [mm/d]	3.11	**2.85**
RMSE [mm/d]	**4.55**	4.72
Medium flows (1 mm/d <= q <= 5mm/d)		
MAE [mm/d]	**0.66**	0.80
RMSE [mm/d]	**0.86**	1.09
Low flows (q < 1mm/d)		
MAE [mm/d]	0.35	**0.20**
RMSE [mm/d]	0.42	**0.34**

566 **Table 2: Model performance in pre-change conditions (1975 – 1979). Bold face numbers**
567 **correspond to the model with superior performance for the particular metric.**

568

569

Hydrol. Earth Syst. Sci. Discuss., https://doi.org/10.5194/hess-2017-382
Manuscript under review for journal Hydrol. Earth Syst. Sci.
Discussion started: 4 July 2017

570

	Sensitivity Index
hl1	0.10
lp	0.12
Maxbas	0.14
fcap	0.18
K0	0.23
K2	0.23
K1	0.38
beta	0.41
perc	0.47

571 **Table 3: Variance Based Sensitivity Analysis Results for HBV parameters: first order sensitivity**
572 **index representing the contribution of varying a single parameter to the variance of the model**
573 **output. Lower values indicate lower sensitivity.**

574

575

576

Hydrol. Earth Syst. Sci. Discuss., https://doi.org/10.5194/hess-2017-382
Manuscript under review for journal Hydrol. Earth Syst. Sci.
Discussion started: 4 July 2017

Hydrology and Earth System Sciences
Discussions

577

Parameters						
	Description	**Units**	**Initial Sampling Distribution**	**Feasible Range**	**Initial s^2 (VVM)**	**Max allowable daily rate of change (LL)**
β	Soil Moisture exponent	[ ]	*N*(2, 0.1)	0 – 7	0.003	$1.8\text{x}10^{-3}$
$fcap$	Maximum soil moisture store depth	[mm]	*N*(467, 10)	10 – 2000	0.003	0.4
$hl1$	Threshold for generation of near surface flow	[mm]	*N*(120, 10)	0 – 400	0.003	0.1
$K0$	Near Surface Flow Routing Coefficient	[ ]	*N*(0.3, 0.005)	0.0625 – 1	0.003	$2\text{x}10^{-4}$
$K1$	Interflow Routing Coefficient	[ ]	$N(0.09, 5\text{x}10^{-4})$	0.02 – 0.1	0.003	$9\text{x}10^{-6}$
$perc$	Percolation rate	[mm/d]	$N(1.3, 10^{-4})$	0 – 3	0.003	10^{-3}
$K2$	Baseflow Routing Coefficient	[ ]	$N(0.01, 10^{-6})$	$5\text{x}10^{-5}$– 0.02	0.003	$9\text{x}10^{-6}$
States						
$sowat$	Soil Moisture Store	[mm]	*N*(0,1)	$(0, fcap)$		
$stw1$	Shallow Layer Store	[mm]	*N*(0,1)	(0, ∞)		
$stw2$	Deep Layer Store	[mm]	*N*(0,0.1)	(0, ∞)		

578 **Table 4: Locally Linear EnKF inputs for the HBV model case**

579

580

581

582

583

584

585

Hydrol. Earth Syst. Sci. Discuss., https://doi.org/10.5194/hess-2017-382
Manuscript under review for journal Hydrol. Earth Syst. Sci.
Discussion started: 4 July 2017

Hydrology and Earth System Sciences
Discussions
Open Access
EGU

Figures

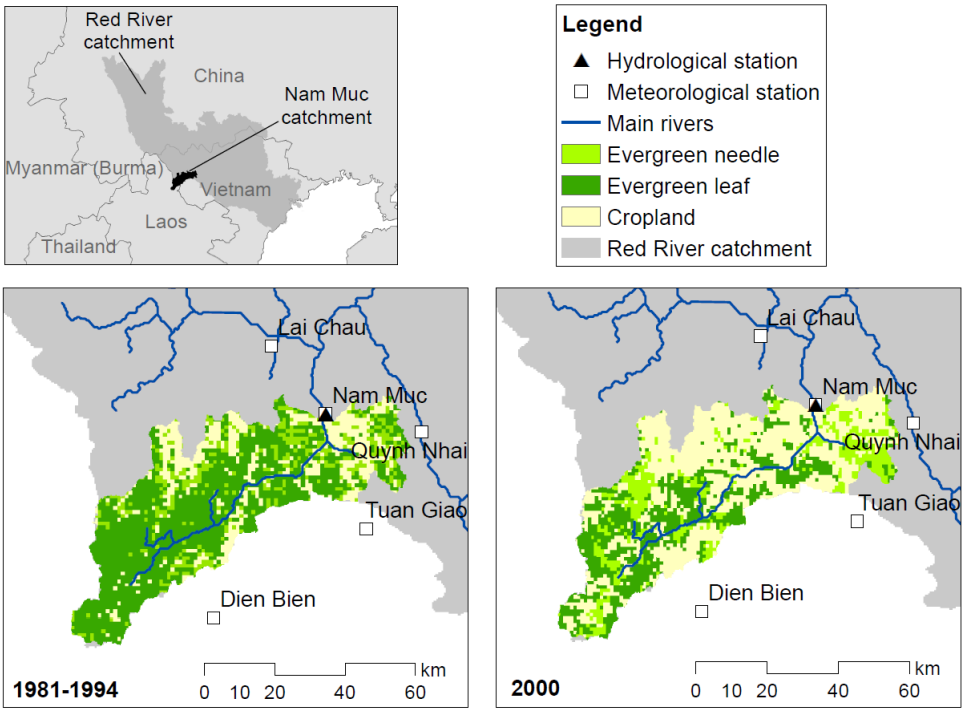

Figure 1: Study Catchment showing gauges and changes in land use cover over time

Hydrol. Earth Syst. Sci. Discuss., https://doi.org/10.5194/hess-2017-382
Manuscript under review for journal Hydrol. Earth Syst. Sci.
Discussion started: 4 July 2017

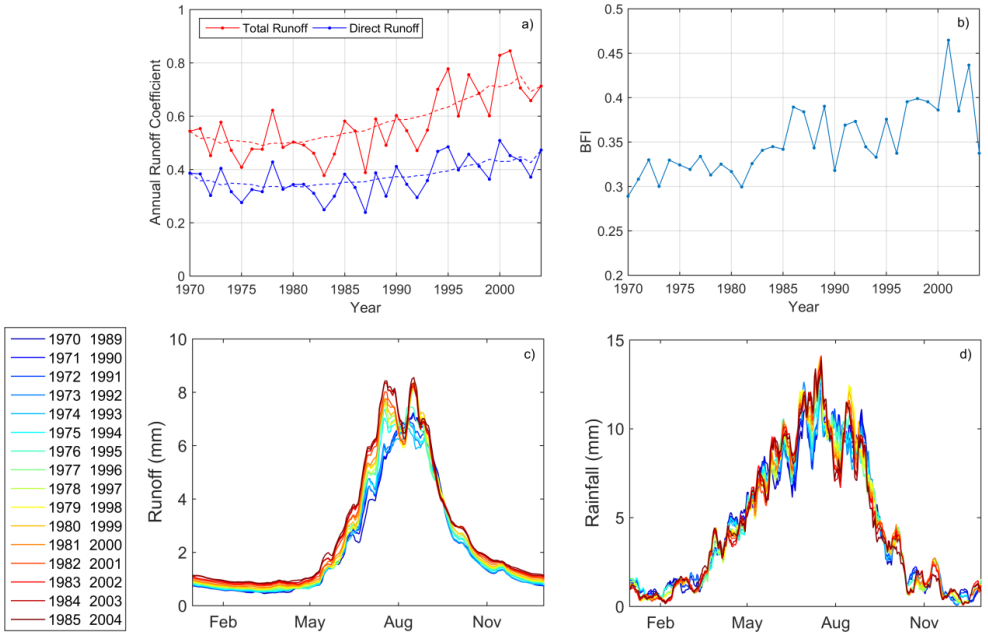

Figure 2: Impact of land use change on observed streamflow: a) Annual Runoff Coefficient, b) Annual Baseflow Index (BFI), c) Moving Average Shifting Horizon (MASH) results for total observed runoff, d) MASH for observed rainfall.

Hydrol. Earth Syst. Sci. Discuss., https://doi.org/10.5194/hess-2017-382
Manuscript under review for journal Hydrol. Earth Syst. Sci.
Discussion started: 4 July 2017

Hydrology and Earth System Sciences
Discussions
Open Access
EGU

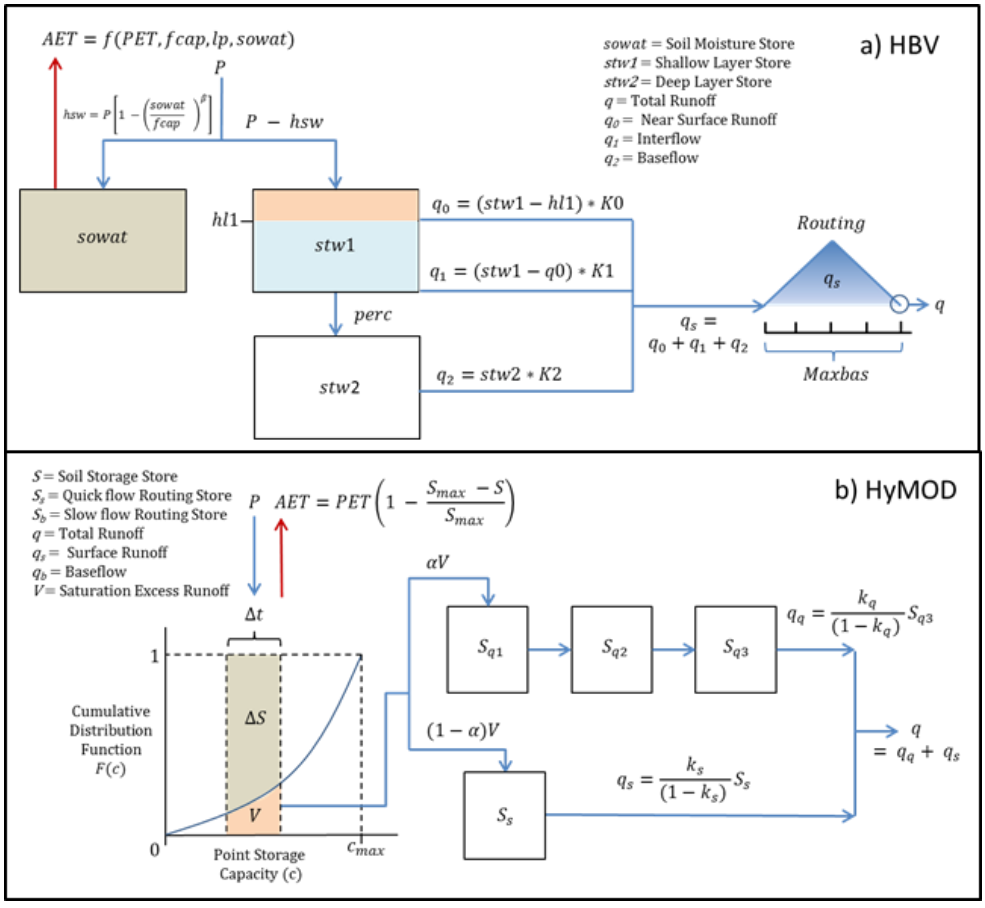

Figure 3. Schematic of the models used in this study: a) HBV and b) HyMOD

Hydrol. Earth Syst. Sci. Discuss., https://doi.org/10.5194/hess-2017-382
Manuscript under review for journal Hydrol. Earth Syst. Sci.
Discussion started: 4 July 2017

Hydrology and Earth System Sciences
Discussions
Open Access
EGU

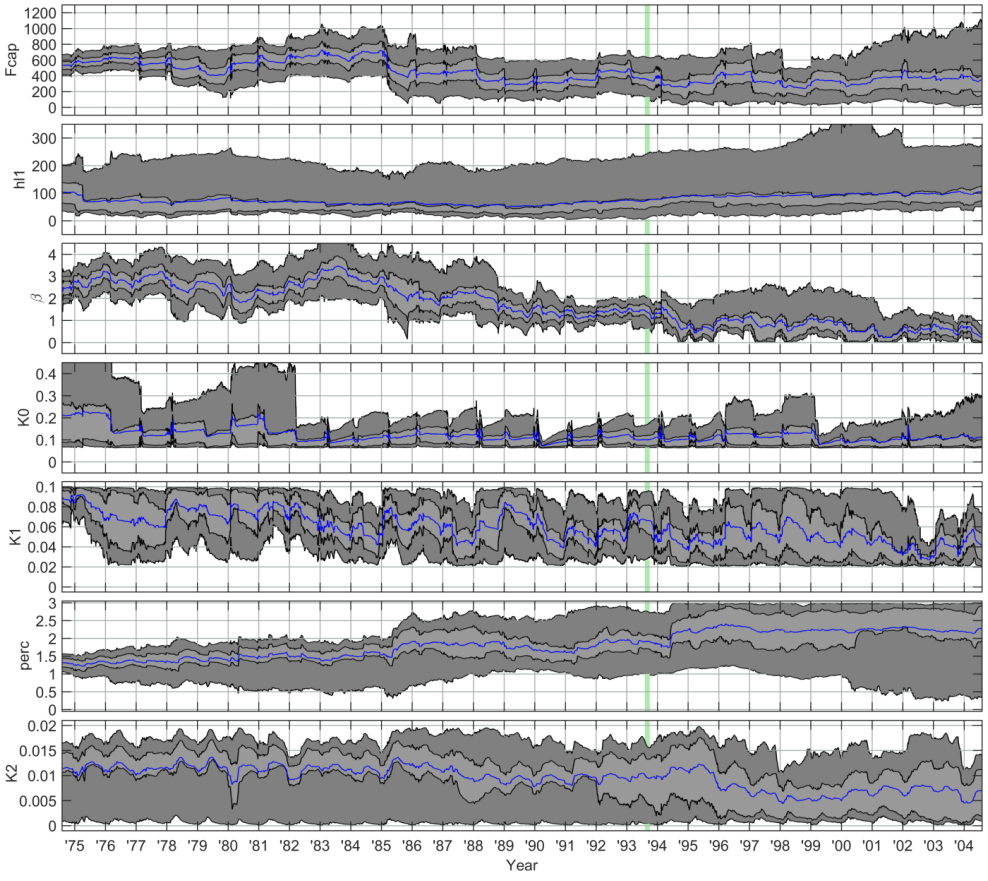

Figure 4: Parameter Trajectories using the HBV model. The dark grey shaded areas indicate the middle 90% of the ensemble, bounded by the 5th and 95th percentiles. The light grey shaded areas indicate the middle 50% of the ensemble, bounded by the 25th and 75th percentiles. The ensemble mean is indicated by the blue line. The vertical green panel indicates the assumed time period of rapid deforestation.

Hydrol. Earth Syst. Sci. Discuss., https://doi.org/10.5194/hess-2017-382
Manuscript under review for journal Hydrol. Earth Syst. Sci.
Discussion started: 4 July 2017

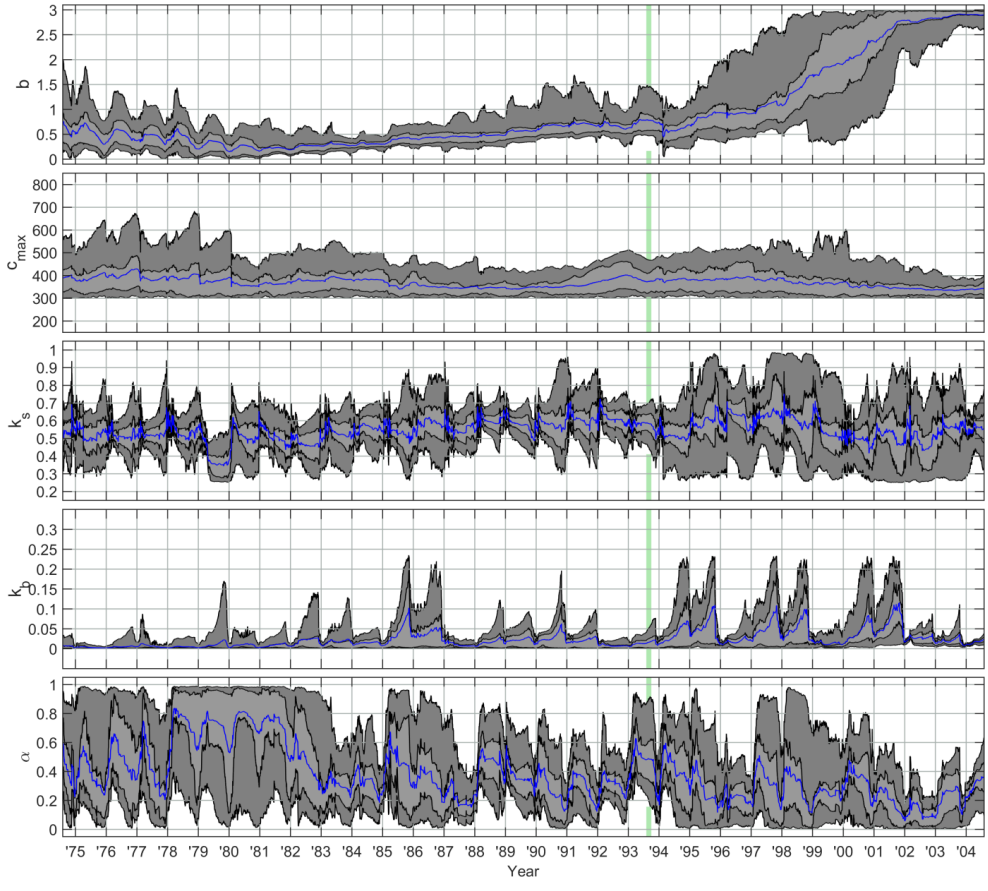

Figure 5: Parameter Trajectories using the HyMOD model. The dark grey shaded areas indicate the middle 90% of the ensemble, bounded by the 5th and 95th percentiles. The light grey shaded areas indicate the middle 50% of the ensemble, bounded by the 25th and 75th percentiles. The ensemble mean is indicated by the blue line. The vertical green panel indicates the assumed time period of rapid deforestation.

Hydrol. Earth Syst. Sci. Discuss., https://doi.org/10.5194/hess-2017-382
Manuscript under review for journal Hydrol. Earth Syst. Sci.
Discussion started: 4 July 2017

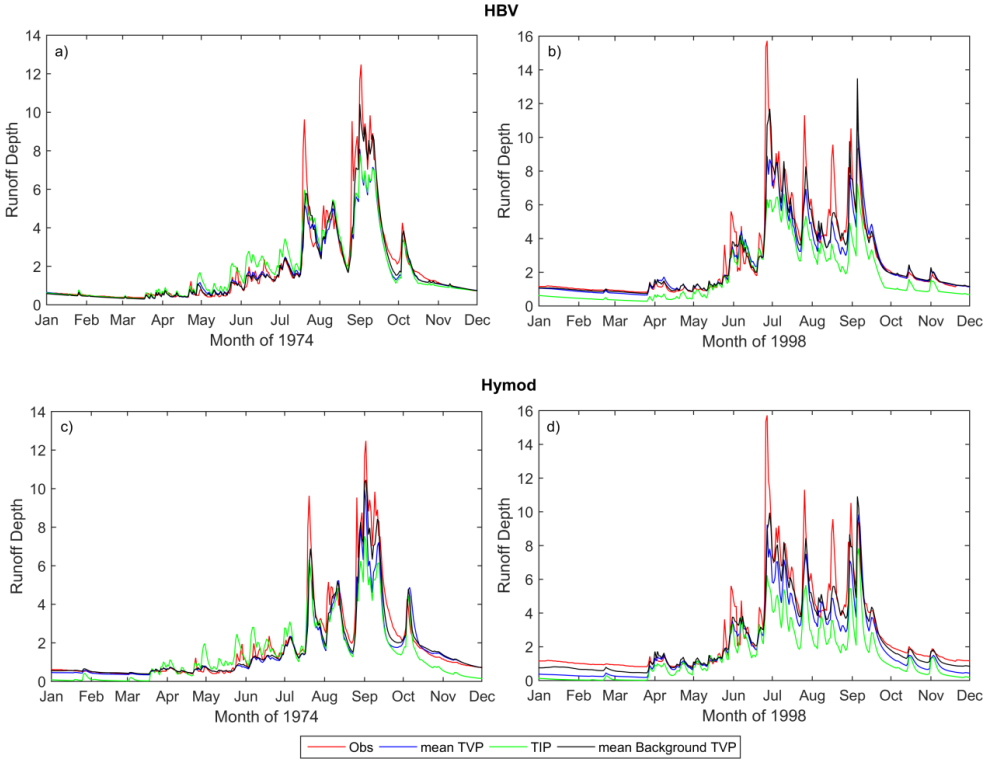

645

646 **Figure 6: Representative Hydrographs of background streamflow from the LL Dual EnKF (black line),**
647 **Time varying parameter model with no state updating (blue line), time invariant parameter model**
648 **with no DA (green line) and observed streamflow (red line). Results for HBV are shown in the top**
649 **row and HyMOD in the bottom row. A pre-change year (1974) is shown on the left and a post**
650 **change year (1998) on the right.**
651

652

653

Hydrol. Earth Syst. Sci. Discuss., https://doi.org/10.5194/hess-2017-382
Manuscript under review for journal Hydrol. Earth Syst. Sci.
Discussion started: 4 July 2017

654

655

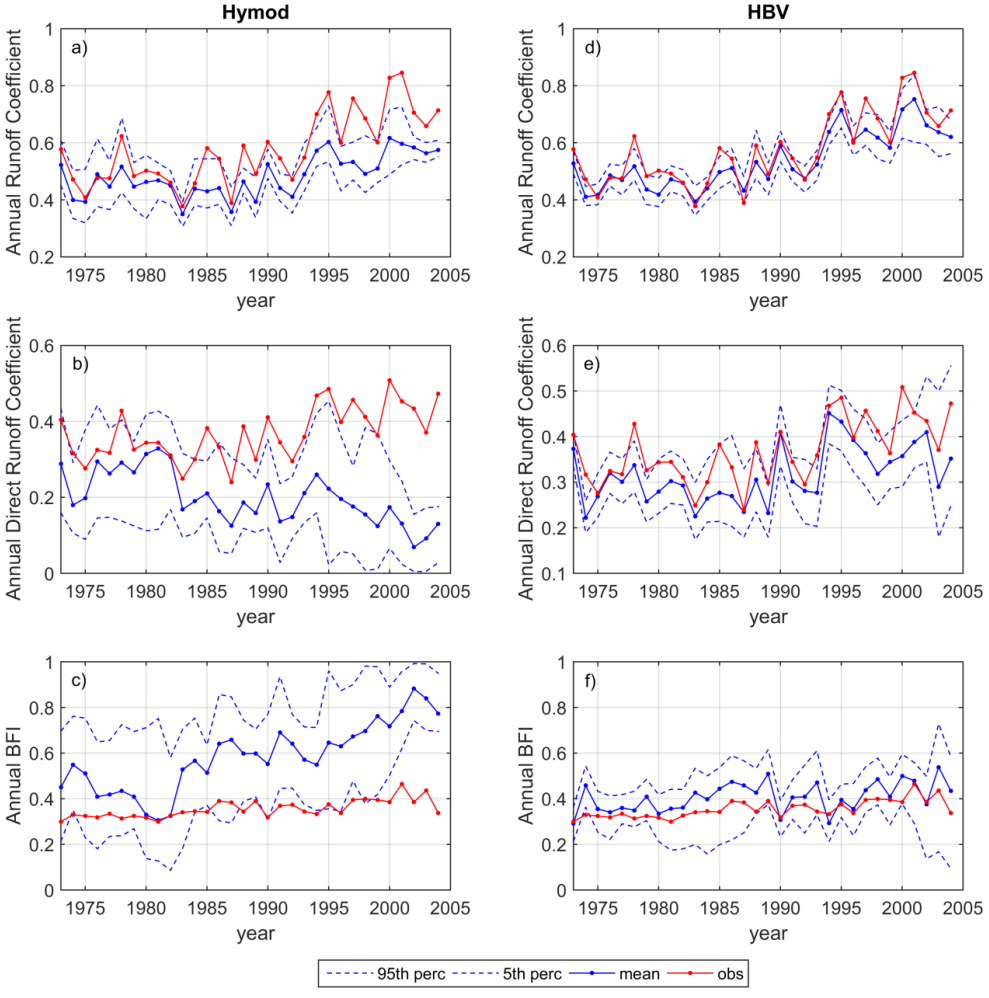

656

657 **Figure 7: Influence of time varying parameters on model output (i.e. without state updating)**
658 **summarized in terms of the Annual Runoff Coefficient (top row), Annual Direct Runoff Coefficient**
659 **(second row) and Annual Baseflow Index (BFI) (third row). Results for HyMOD are shown in the**
660 **first column, HBV are shown in the second column.**
661

662

663

664

Hydrol. Earth Syst. Sci. Discuss., https://doi.org/10.5194/hess-2017-382
Manuscript under review for journal Hydrol. Earth Syst. Sci.
Discussion started: 4 July 2017

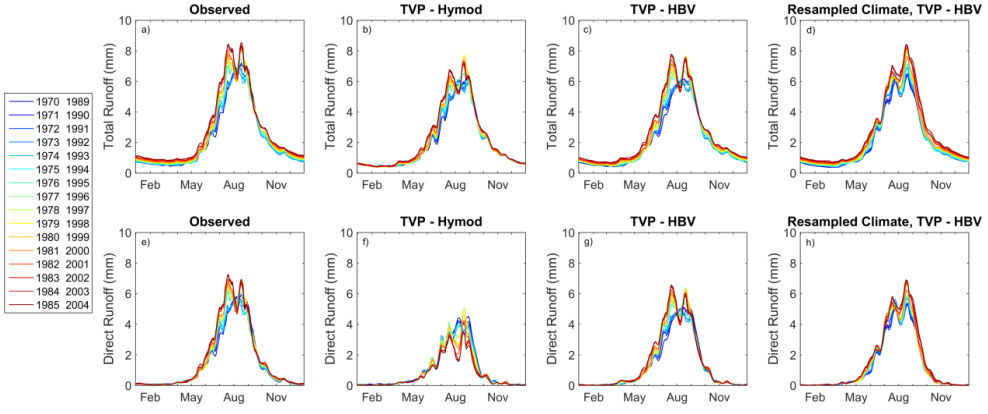

Figure 8: Moving Average Shifting Horizon (MASH) results for observed streamflow (first column), simulated streamflow from time varying parameter model (without state DA) for HYMOD (2nd column), HBV (third column), resampled climate HBV (fourth column). These are split into total runoff (first row) and direct runoff or surface runoff (2nd row).